RESEARCH ARTICLE

Managing aquifer recharge with multi-source water to realize sustainable management of groundwater resources in Jinan, China

Zhengxian Zhang[1,2] · Weiping Wang[3]

Abstract
Managed aquifer recharge (MAR) is an important approach to address water security, water quality decline, ground subsidence, and aquifer degradation. In this study, the large-scale recharge experiments were conducted in a natural river with multiple water sources. The MAR with multi-source water was investigated by developing an improved matter-element model under a limited recharged quantity and period in Jinan, China. Results showed that the background levels (BL) of groundwater quality before recharge was relatively good. However, the use of different water sources would cause a significant increase in the content of some groundwater quality indexes, which might further induce deterioration of regional groundwater quality. And the water quality in porous and karst aquifer displayed deteriorating trends during different water source recharge. Additionally, the adverse effects of recharge water sources on regional groundwater quality in turn was South-to-North Water Diversion Project (SN) > Yellow River (YR) > Wohushan Reservoir (WR). Meanwhile, the high-risk indexes in groundwater quality were presented during different water source recharge. Accordingly, relevant suggestions and measures were then put forward to optimize the MAR with multi-source water and explore the high-efficiency and low-risk recharge mode.

Keywords Managed aquifer recharge · Artificial recharge · Multi-source water · Improved matter-element model · Groundwater quality

Introduction

Managed aquifer recharge (MAR) was an increasingly common measure for increasing urban water supply and sustaining water resilience (Dillon 2005; Rodríguez-Escales et al. 2017). Excess water was stored in the aquifers for future consumption by MAR. And the major methods used for MAR include bank filtration, well injection, rainwater harvesting, and infiltration ponds (Ebrahim et al. 2016; Ganot et al. 2017). MAR provided a series of technical solutions to sustainably manage water resources by not only recharging groundwater but also displaying an integrated vision of water resources, following the EU Water Framework Directive approach (Escalante et al. 2019). The groundwater level dropped rapidly over 10 m per year in China. And groundwater overexploitation had occurred in 164 areas of China's 31 provinces, affecting more than 180,000 km^2 (Werner et al. 2013). Groundwater funnel formed gradually and expanded by the groundwater depletion, which caused frequent land subsidence, water quality deterioration, and seawater intrusion. To alleviate the abovementioned issues, a series of water management measures had been carried out in China, such as improving irrigation technology and water efficiency, implementing water price reforms, and water use rights. However, the lack of detailed information on the amount of groundwater extracted, and limited groundwater monitoring wells, as well as complex recharge water sources, make groundwater management still face severe challenges.

✉ Weiping Wang
stu_wangwp@ujn.edu.cn; wangweipingwp@126.com

1   State Key Laboratory of Water Resources and Hydropower Engineering Science, Wuhan University, Wuhan 430072, China

2   State Key Laboratory of Hydrology-Water Resources and Hydraulic Engineering, Nanjing Hydraulic Research Institute, Nanjing 210029, China

3   School of Water Conservancy and Environment, University of Jinan, Jinan 250022, China

Water security associated with groundwater overexploitation was increasingly becoming a critical environmental concern. Growing studies had indicated that MAR could effectively improve water supply and surface water quality. Rainwater quality after being treated by constructed wetlands and MAR was studied in urban catchments (Page et al. 2010). The mechanism of excessive air formation during MAR (natural bank filtration) was investigated in Berlin (Massmann and Sültenfuß 2008). Leonard et al. (2015) analyzed the possibility of MAR-treated rainwater for potable and non-potable. Mankad et al. (2015) qualitatively studied the acceptance of MAR-treated urban rainwater for household use combined with psychological and policy-related factors. MAR risks were revealed using fault tree and probabilistic assessment methods at six recharge sites in the Mediterranean Basin (Rodríguez Escales et al. 2018). Fiorillo et al. (2019) analyzed the features of MAR in the Caposele Spring area, southern Italy, using a daily recharge model. MAR projects of two demonstration sites were studied according to the monitoring data in the Guadiana Basin, Spain (Fernández Escalante 2015). The 150,000-m^3/day MAR project was proposed as an economic solution to solve the water supply and groundwater quality issues in Southwestern Florida, USA (Missimer et al. 2017). Dillon et al. (2019) assessed the efficacy of MAR and illustrated the development of MAR at the global scale over the past 60 years. To investigate the hydrodynamics of unsaturated flow and recharge efficiency, Liang et al. (2018) proposed a mathematical method for MAR induced by a Vadose zone infiltration well. Groundwater quality during MAR was sampled and monitored regularly at the Krasnohorska karst system in Slovakia (Malík et al. 2020). Urrutia et al. (2019) investigated the contribution of snowmelt and rainfall to aquifer recharge in the Andean Cordillera of northern Chile. Yin et al. (2011) analyzed the sustainable yield of karst water in Huaibei, China, using an artificial neural network model. The MAR system in karst spring catchment was simulated using the latest research version of MODFLOW-CFP (Xu et al. 2015). The influences of an inter-basin surface water transfer project on the MAR system and groundwater ecosystem were evaluated using a numerical simulation model in arid northwestern China (Zhu et al. 2018). Gong et al. (2016) developed a salt balance model in Badain Jaran Desert, China, to evaluate the salt accumulations in the groundwater-fed lakes. Lysimeter measurement and soil moisture models were used in the Huaihe River plain, China, to estimate groundwater recharge caused by precipitation and groundwater loss (Chen et al. 2008). The effects of clogging and dissolution in the MAR system were explored using hydrogeochemical and numerical simulation methods (Du et al. 2013; Ye et al. 2019).

Jinan is famous for its spring water and has been hailed as "Spring City." The abundant spring water resources have made tremendous contributions to the socio-economic development in Jinan. Recently, the contradictions between water supply and demand have become increasingly prominent, with the rapid urbanization and increasing urban population (Jiao et al. 2017). In this case, Jinan has to exploit local groundwater to address the current situation of water shortages. However, a continuous decrease has occurred in groundwater level and free outflow rate of springs due to long-term overexploitation of urban groundwater resources (Wang et al. 2019). This situation has progressively become major threats to the protection of spring water resources and the safety of urban water supply in Jinan (Wang et al. 2017a, b). To realize the sustainable management of groundwater resources, it was urgent to carry out the MAR project in Jinan.

The aquifer system in Jinan spring catchment is a heterogeneous system, and the relationship between replenishment and discharge is extremely complex (Wang et al. 2015a, b; Gao and Tian 2018). And numerous empirical studies associated with groundwater management had been conducted in Jinan. The three-dimensional geological models were established to investigate the hydrogeological structure and groundwater flow characteristics in Jinan (Wu and Xu 2005; Kang et al. 2011; Wang et al. 2016; Luo et al. 2020). Qi et al. (2016) used the wavelet analysis method to predict the groundwater table in the Jinan spring catchment and then proposed sustainable groundwater extraction. To optimize the layout of groundwater recharge and extraction, the hydraulic connectivity in the Jinan spring catchment was explored (Wang et al. 2017a, b; Zhang et al. 2018). Hydrochemistry ions were used to study the recharge and discharge controls and groundwater flow paths in the Jinan spring catchment (Zhang et al. 2017b; Xing et al. 2018). Environmental isotope tracer tests were employed to investigate the main recharged water source for the Jinan spring catchment (Yin et al. 2017; Gao et al. 2014).

The aforementioned studies had achieved promising results and laid the foundation for optimizing regional MAR operations and maintaining water resilience. Although numerous micro and macro studies on MAR have been conducted, some investigations associated with multiple recharge water sources were scarce during the MAR process. Additionally, most current researches focus on the hydrogeochemistry of groundwater, almost ignoring the change in the state of groundwater quality. And there were few quantitative studies on the combination of comprehensive evaluation and high-risk indexes in groundwater quality. Therefore, it was necessary to investigate the impact of MAR with multi-source water on groundwater quality, especially in Jinan with groundwater depletion.

To achieve sustainable management of groundwater in Jinan, this study quantitatively investigated the impact of multi-source MAR on groundwater quality and high-risk indexes. The large-scale recharge experiments using multiple water sources were conducted in a natural river that the riverbed has high permeability.

Groundwater and recharge water sources were sampled and tested to quantify the adverse effects of different recharge water sources on local groundwater quality, under a limited recharged quantity and period. An improved matter-element model was developed to implement a comprehensive assessment of groundwater quality, and the high-risk indexes in groundwater quality were determined during different water source recharge. The combination of two methods provides a new approach to investigate the MAR with multi-source water from multiple angles (the overall situation and high-risk indexes in groundwater quality). We hope this method could be extended to other MAR with multi-source water to optimize the operation of groundwater replenishment and reduce the damage of the recharged water source on the local aquifer system. Accordingly, the effects of MAR with multi-source water were assessed from the perspective of groundwater quality control, and countermeasures were then developed to provide a basis for formulating the high-efficiency and low-risk MAR mode.

Study area

Jinan spring catchment and Yufu River

Jinan's terrain slopes from the south to the north with an elevation difference of more than 500 m (Yu et al. 2014). This unique geological structure makes the surface water and groundwater in Mount Tai flow into the northern urban area. Large quantities of groundwater are blocked by impermeable igneous rocks to form the high water pressure zones in northern Jinan (Xie 2017). After that, the groundwater flows out to form the Jinan spring groups under the action of strong water pressure (Fig. 1). As a symbol of Jinan's social culture, the Jinan spring groups have made a historical contribution to the economic prosperity (Zhang et al. 2017a).

To alleviate the pressure of spring water protection and urban water supply, the MAR projects in Yufu River have been carried out in Jinan. And the surface water in the Wohushan Reservoir (WR), the Yellow River (YR) and the South-to-North Water Diversion Project (SN) are used as the water sources for MAR, respectively. These MAR projects have played important roles in replenishing local groundwater and maintaining higher groundwater level of the Jinan spring groups. Although the MAR projects have been gradually implemented, there are still some challenges and obstacles. Due to the different recharge water sources and relatively complicated geological structure in Jinan, how to efficiently replenish local groundwater, avoid groundwater pollution, and sustain water resilience are the critical links.

Existing MAR projects in Yufu River

Yufu River is located in western Jinan. It originates from the mountain streams of Jinxiu, Jinyang, and Jinyun in the mountainous area of southern Jinan (Fig. 2). The rainfall and mountain streams are collected into the Wohushan Reservoir, and the Yufu River is then formed by the Wohushan Reservoir release (Hou et al. 2016). The study area is located in the upper reaches of the Yufu River. The riverbeds and river floodplains are mainly composed of loose Quaternary sediments (gravel, sand, and clay) with a thickness of about 24 m. And the strata are mainly Cambrian limestone with a thickness of about 150 m. This part of the Yufu River has a high perviousness based on its fully developed karst conditions. Consequently, the Yufu River plays an important role in groundwater replenishment and urban water supply in Jinan. Currently, the MAR projects in the Yufu River mainly include the following: (i) Yufu River is replenished by the WR release, and the water source of this MAR project is the local surface water in WR; (ii) surface water from YR is transferred to the upper reaches of Yufu River through the pumping station, and water source of this MAR project is from the YR; and (iii) surface water from the Jiping Main Canal is transported into the upper reaches of Yufu River employing water pipes, and water source of this MAR project is from the SN. The aforementioned MAR projects in Yufu River are shown in Fig. 2.

The water source and recharge quantity of MAR projects

As shown in Table 1, the water sources of MAR were from the WR, YR, and SN, respectively. The water quality and quantity of recharge water sources are two main reasons for groundwater quality changes after MAR. The recharge quantity was 1120–1170 ($10^4 m^3$) and the recharge period was from December to March of the next year in 2015–2018. Recharge quantity and period were well controlled in this study. So, the groundwater quality changes after recharge were mainly subjected to the water quality of recharge water source.

Monitoring wells and groundwater sampling

Eight monitoring wells (W1–W8) along the upper reaches of Yufu River were selected to monitor the groundwater quality. These monitoring wells consisted of three wells (W1–W3) in porous aquifer and five wells (W4–W8) in karst aquifer (Fig. 3). The depth of monitoring well was 24 m and 150 m in porous medium formation and karst formation, respectively. To determine the background level (BL) of groundwater quality, the groundwater in each monitoring well was sampled to test its water quality before MAR. Groundwater was directly sampled from a specific depth using the Discrete
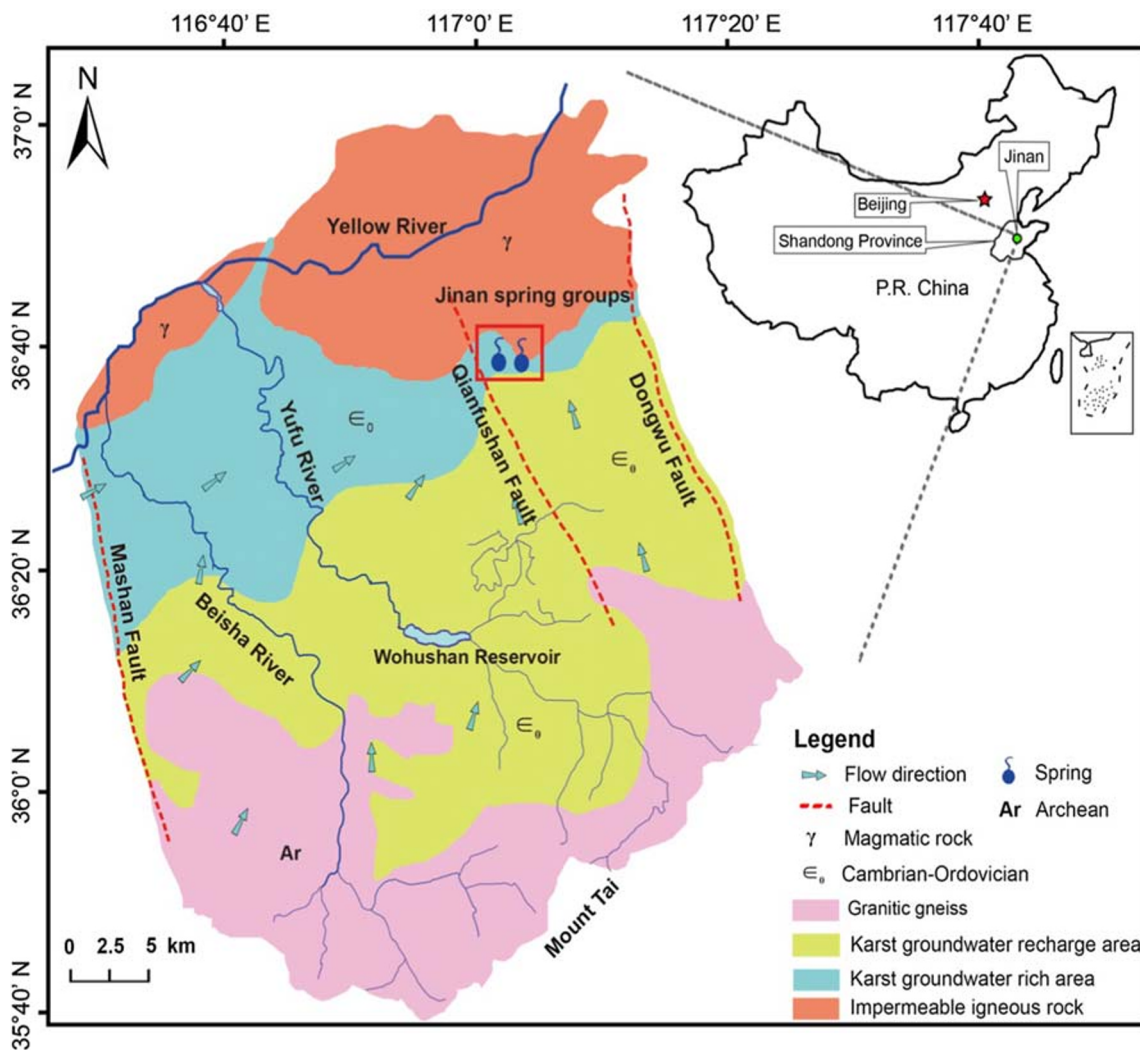
Fig. 1 Jinan spring catchment and Yufu River (Zhang et al. 2018)

Interval Sampler, Model 425 (Solinst Canada Ltd., Georgetown, Ontario, Canada), and collected water could be highly representative of groundwater surrounding the monitoring well at that level (Parker and Clark 2004). The Discrete Interval Sampler was a passive sampler and was pressurized when lowered and upon retrieval to prevent water mixing at different levels (Dermatas et al. 2015). Furthermore, the water quality conditions of recharge water sources (WR, YR, and SN) were obtained through the sampling analysis.

Materials and methods

Index system

Groundwater quality data from eight monitoring wells were served as the evaluation indexes. Environmental Quality Standards for Groundwater, China (GB/T14848-2017), were used as the evaluation standards. The groundwater quality was regularly sampled and tested from 2015 to 2018 during different water source recharge process. The test results showed that some water quality indexes in pore and karst water were detected, including total hardness (TH), nitrite nitrogen (NO_2-N), nitrate nitrogen (NO_3-N), ammonia nitrogen (NH_4^+), chlorides (Cl^-), fluoride (F^-), sulfate (SO_4^{2-}), sodium ions (Na^+), permanganate index (COD_{Mn}), pondus hydrogenii (PH), turbidity (TUB), and total dissolved solids (TDS). Previous research in Yufu River indicated that other groundwater quality indexes listed by Environmental Quality Standards for Groundwater, China (GB/T14848-2017), had less content or had not been detected in the study area, in addition to the above twelve groundwater quality indexes (Li et al. 2017b). So, the index system of groundwater quality was constructed using the above twelve indexes. The grades of groundwater quality were divided into five classifications (I, II, III, IV, and
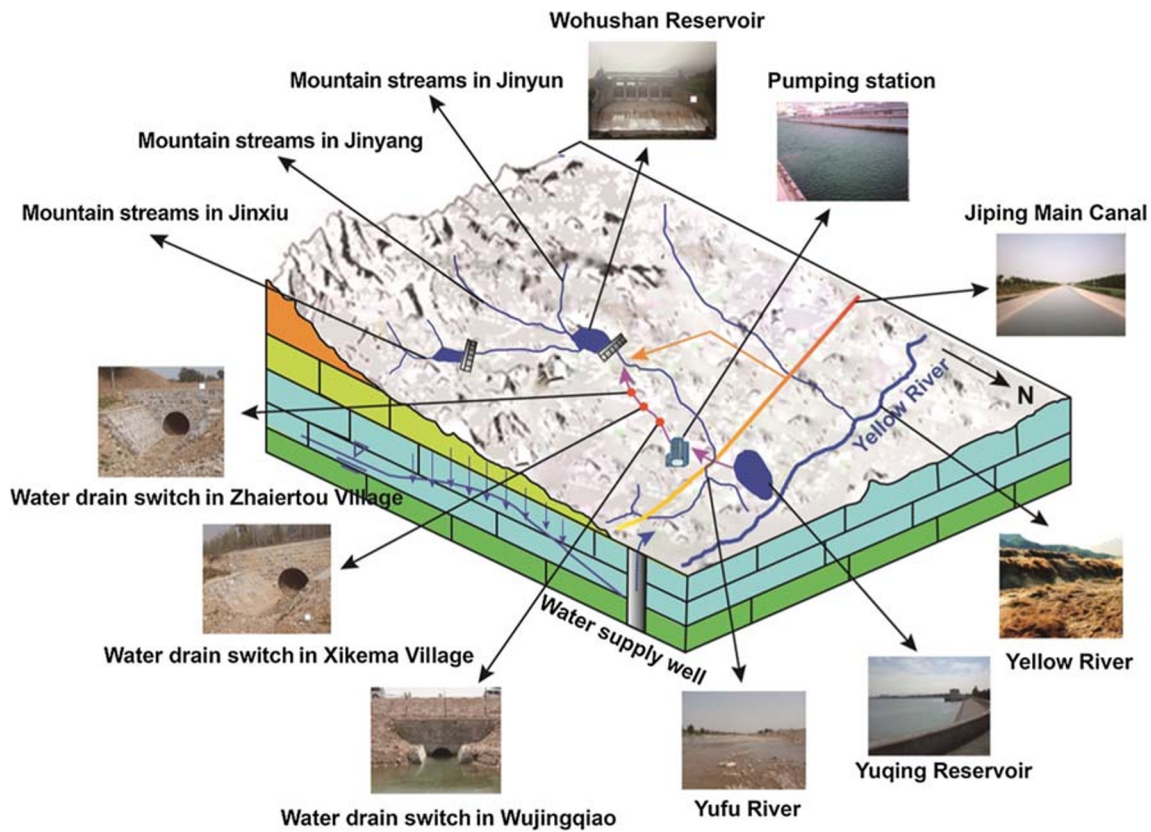
Fig. 2 Existing MAR projects in Yufu River

V) based on Environmental Quality Standards for Groundwater, China (GB/T14848-2017). Classifications of evaluation indexes are displayed in Table 2.

Improved matter-element model

Matter-element model was presented by the Chinese researcher Cai Wen in 1983 (Cai 1999). Rules and methods for solving specific problems were qualitatively and quantitatively investigated according to the formalized logic tools (Li et al. 2017a; Liu et al. 2019). The matter-element method was the theoretical foundation, the logical unit was the matter-element, and a matter-element model was then developed by the characteristics and characteristic values of the evaluation object (Liu and Zou 2012). This model can quantify qualitative

indexes and also deal well with the diverse and ambiguous evaluation objects.

Determination of the classical field, controlled field, and matter-element

The evaluation object N has a characteristic c with the value of v. The ordered triple $R = (N, c, v)$ is composed of N, c, and v, which serves as the basic element for describing things. R is called the matter-element, and the three elements N, c, and v are used to establish the basis for matter-element theory. Assume that the object N can be described by m characteristics c_1, c_2, $\cdots$, c_m, and the corresponding characteristic values are v_1, v_2, $\cdots$, v_m. At this point, R is an m-dimensional matter-element, and defined as follows:

Table 1 Recharge water source and quantity in Yufu River from 2015 to 2018

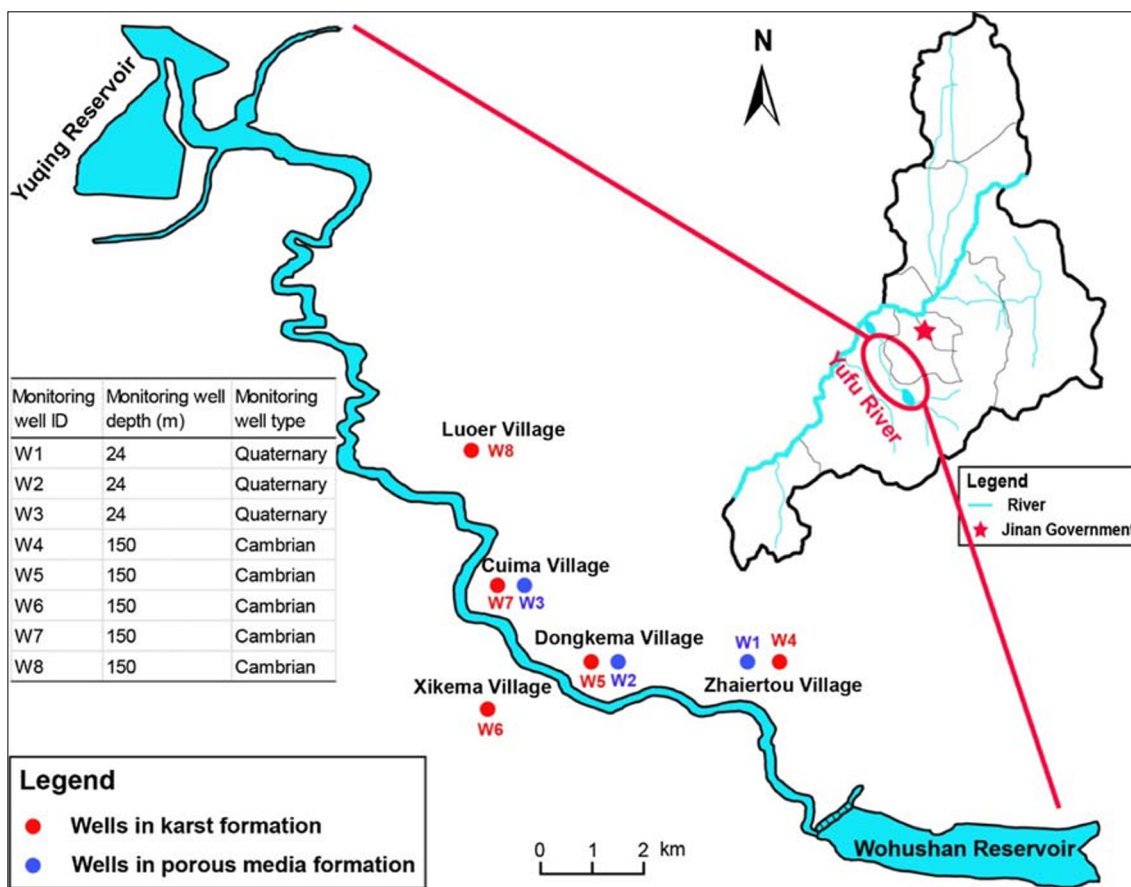| Year	Recharge water source	Recharge period	Sampling time	Recharge quantity ($10^4 m^3$)
2015–2016	YR	December to March of next year	March 2016	1170
2016–2017	WR	December to March of next year	March 2017	1120
2017–2018	SN	December to March of next year	March 2018	1140

Fig. 3 The monitoring wells in Yufu River

$$R = (N, C, V) = \begin{bmatrix} R_1 \\ R_2 \\ \vdots \\ R_m \end{bmatrix} = \begin{bmatrix} N & c_1 & v_1 \\ & c_2 & v_2 \\ & \vdots & \vdots \\ & c_m & v_m \end{bmatrix} \quad (1)$$

where R is the matter-element, R_i is the sub-matter-element of R, N is the evaluation object, $C = [c_1, c_2, \cdots, c_m]$ is the eigenvector, $V = [v_1, v_2, \cdots, v_m]$ is the value corresponding to the eigenvector.

Table 2 Grades of groundwater quality in Environmental Quality Standards for Groundwater, China (GB/T14848-2017)

Index	Unit	Grades of groundwater quality				
		I	II	III	IV	V
TH (C_1)	(mg/L)	(0, 150)	(150, 300)	(300, 450)	(450, 650)	≥ 650
NO$_2$-N (C_2)	(mg/L)	(0, 0.01)	(0.01, 0.1)	(0.1, 1)	(1, 4.8)	≥ 4.8
NO$_3$-N (C_3)	(mg/L)	(0, 2)	(2, 5)	(5, 20)	(20, 30)	≥ 30
NH$_4^+$ (C_4)	(mg/L)	(0, 0.02)	(0.02, 0.1)	(0.1, 0.5)	(0.5, 1.5)	≥ 1.5
Cl$^-$ (C_5)	(mg/L)	(0, 50)	(50, 150)	(150, 250)	(250, 350)	≥ 350
F$^-$ (C_6)	(mg/L)	(0, 1)	(0, 1)	(0, 1)	(1, 2)	≥ 2
SO$_4^{2-}$ (C_7)	(mg/L)	(0, 50)	(50, 150)	(150, 250)	(250, 350)	≥ 350
Na$^+$ (C_8)	(mg/L)	(0, 100)	(100, 150)	(150, 200)	(200, 400)	≥ 400
COD$_{Mn}$ (C_9)	(mg/L)	(0, 1)	(1, 2)	(2, 3)	(3, 10)	≥ 10
PH (C_{10})	1	(6.5, 8.5)	(6.5, 8.5)	(6.5, 8.5)	(8.5, 9)	(9, 14)
TUB (C_{11})	(NTU)	(0, 3)	(0, 3)	(0, 3)	(3, 10)	≥ 10
TDS (C_{12})	(mg/L)	(0, 300)	(300, 500)	(500, 1000)	(1000, 2000)	≥ 2000

Suppose:

$$
R_j = \begin{bmatrix} N_j & c_1 & v_{j1} \\ & c_2 & v_{j2} \\ & \vdots & \vdots \\ & c_n & v_{jn} \end{bmatrix} = \begin{bmatrix} N_j & c_1 & [a_{j1},b_{j1}] \\ & c_2 & [a_{j2},b_{j2}] \\ & \vdots & \vdots \\ & c_n & [a_{jn},b_{jn}] \end{bmatrix} \quad (2)
$$

where N_j represents j evaluation grades, $c_1, c_2, \cdots, c_n$ are the characteristics of N_j, $v_{j1}, v_{j2}, \cdots, v_{jn}$ are the value ranges corresponding to the $c_1, c_2, \cdots, c_n$, and $v_{ji}(v_{ji} = [a_{ji},b_{ji}])$ is called the classical field.

Similarly,

$$
R_P = \begin{bmatrix} P & c_1 & v_{p1} \\ & c_2 & v_{p2} \\ & \vdots & \vdots \\ & c_n & v_{pn} \end{bmatrix} = \begin{bmatrix} P & c_1 & [a_{P1}, b_{P1}] \\ & c_2 & [a_{P2}, b_{P2}] \\ & \vdots & \vdots \\ & c_n & [a_{pn}, b_{pn}] \end{bmatrix} \quad (3)
$$

where P is all the grades in evaluation objects, $v_{p1}, v_{p2}, \cdots, v_{pn}$ are the value ranges corresponding to the $c_1, c_2, \cdots, c_n$, and v_{Pi} ($v_{pi} = [a_{pi},b_{pi}]$) is called the controlled field of P.

The evaluation objects are represented by the matter-element.

$$
R_0 = \begin{bmatrix} P_0 & c_1 & v_1 \\ & c_2 & v_2 \\ & \vdots & \vdots \\ & c_n & v_n \end{bmatrix} \quad (4)
$$

where R_0 is the matter-element to be evaluated, $v_1, v_2, \cdots, v_n$ are the specific data of P_0 about $c_1, c_2, \cdots, c_n$.

Calculation of the combined weights

The conventional combined weighting methods include multiplication and linear normalization. And they often have some limitations, such as the multiplication normalization method is only applicable to the cases where the number of indexes is large and the weight distribution between indexes is relatively uniform (Wang et al. 2009; Tang and Zhang 2013). It is difficult to determine accurately the preference coefficient of the linear weighting method, and it is usually applied based on experiences (Liu et al. 2020a, b; Zhang and Li 2020). To overcome these primary imperfections of conventional weighting methods, we propose a new combined weighting method based on the advantages of the subjective and objective weighting methods. There are two issues needed to be considered behind this combined weight. In the first place, the decision-makers' preference for index attributes should be considered. The other point is that the information content provided by data itself should be used as much as possible. In view of this, the combined weighting method was proposed to make the weights and decision results become more reliable in the decision-making process. Detailed steps were as follows.

(i) Definition of ideal solution

Assume that the weights of evaluation indexes obtained by subjective weighting method (analytic hierarchy process (AHP)) are $u = (u_1, u_2, \ldots, u_n)$, and the weights obtained by objective weighting method (information entropy) are $h = (h_1, h_2, \ldots, h_n)$, along with the combined weights obtained by the ideal solution method are $w = (w_1, w_2, \ldots, w_n)$.

(ii) Deviations of different weighting methods

Unitization of weight vectors can be expressed as:

$$
u_j' = \frac{u_j}{\sqrt{u_1^2 + u_1^2 + \cdots + u_n^2}}; \ h_j' = \frac{h_j}{\sqrt{h_1^2 + h_1^2 + \cdots + h_n^2}}; \quad (5)
$$
$$
w_j' = \frac{w_j}{\sqrt{w_1^2 + w_1^2 + \cdots + w_n^2}}
$$

(iii) Calculation of combined weight

$w_1', w_2', \cdots, w_n'$ can be obtained according to Eq. (6).

$$
w_j' = \left[\frac{u_j'^2 + h_j'^2}{2} \right]^{\frac{1}{2}} \quad (6)
$$

Normalizing $w_1', w_2', \cdots, w_n'$ to get the combined weight w_j, the formula can be expressed as:

$$
w_j = \frac{w_j'}{\sum\limits_{j=1}^{n} w_j'}, (j = 1, 2, \cdots n) \quad (7)
$$

A detailed derivation process of the above model is described in the Supplementary Material.

Calculation of variable eigenvalues

The distance between matter-element and classical field is derived with Eq. (8).

$$
\rho_{(x_0, v_{ji})} = \left| x_0 - \frac{1}{2} (a_{ji} + b_{ji}) \right| - \frac{1}{2} (b_{ji} - a_{ji}) \quad (8)
$$

where $\rho_{(x_0, v_{ji})}$ is the distance between matter-element and classical field, x_0 is the point value on the real axis, a_{ji} and b_{ji} are the left and right endpoints of interval v_{ji}, respectively.

(i) Calculation of the comprehensive correlation degree (CCD)

The correlation function between evaluated matter-element and each grade can be established by Eq. (9).

$$K_j(x_0) = \begin{cases} \dfrac{\rho_{(x_0,v_{ji})}}{\rho_{(x_0,v_{Pi})} - \rho_{(x_0,v_{ji})}} & x_0 \notin v_{ji} \\ -\dfrac{\rho_{(x_0,v_{ji})}}{|v_{ji}|} & x_0 \in v_{ji} \end{cases} \qquad (9)$$

where $K_j(x_0)$ expresses the value of correlation function for evaluated index x_0 related to the jth grade, $\rho_{(x_0,v_{ji})}$ represents the distance between the evaluated matter-element of index x_0 and the interval v_{ji} in the classical field, $\rho_{(x_0,v_{pi})}$ is the distance between the evaluated matter-element of index x_0 and the interval v_{pi} in the controlled field, and $|v_{ji}|$ ($|v_{ji}| = |b_{ji} - a_{ji}|$) is the value range of the jth grade in the classical field.

Correlation function $K_j(x_i)$ is replaced by CCD.

$$K_j(P_0) = \sum_{i=1}^{n} w_i K_j(x_i) \qquad (10)$$

where $K_j(P_0)$ expresses the CCD of evaluated matter-element P_0 related to the jth grade, w_i is the combined weight of evaluated indexes, $K_j(x_i)$ is the correlation function of the ith evaluated index related to the jth grade.

(ii)　Grade rating and variable eigenvalues calculation

If $K_{j0}(P_0) = \max K_j(P_0)$, ($j = 1, 2, …, m$), then we conclude that the evaluated matter-element P_0 belongs to the grade j_0.

The comprehensive grade of the evaluation object can be determined by $\overline{K_j}(P_0)$ set.

$$\overline{K_j}(P_0) = \frac{K_j(P_0) - \min_{1 \le j \le m} K_j(P_0)}{\max_{1 \le j \le m} K_j(P_0) - \min_{1 \le j \le m} K_j(P_0)} \qquad (11)$$

where $\overline{K_j}(P_0)$ is the CCD corresponding to the jth grade, $\min_{1 \le j \le m} K_j(P_0)$ and $\max_{1 \le j \le m} K_j(P_0)$ are the minimum and maximum values of CCD in all grades, respectively.

The variable eigenvalue (VE) of matter-element P_0 is:

$$j^* = \frac{\sum_{j=1}^{m} j \cdot \overline{K_j}(P_0)}{\sum_{j=1}^{m} \overline{K_j}(P_0)} \qquad (12)$$

where j is the evaluated comprehensive grade, j^* is the VE of matter-element P_0, and j^* can be used as a reference for distinguishing the degree of the evaluated matter-element tend to adjacent grade.

Results

Hydrochemical types in MAR water source and BL of groundwater

The main ion compositions in MAR water source and BL of groundwater were analyzed using the Piper diagram (Fig. 4). The most abundant ions in BL of pore and karst water were Ca^{2+} that accounted for 60–70% of the total cation content, and HCO_3^- that was up to 70–80% of the total anion content. Accordingly, the hydrochemical type in BL of groundwater was of the HCO_3-Ca type. This indicated that the ion compositions of groundwater were single before MAR, and the BL were relatively good in the study area. Compared with the ion compositions of BL, the ion changes in WR and YR primarily included that the Ca^{2+} and HCO_3^- content was decreased, and the Mg^{2+} and SO_4^{2-} content was increased. In light of this, the hydrochemical type in WR and YR was of the $HCO_3 \cdot SO_4$-$Ca \cdot Mg$ type. When the SN was used as MAR water source, the most abundant cation was Na^+ that accounted for 50–60% of the total cation content, and the relatively abundant anions were HCO_3^-, Cl^- and SO_4^{2-}. So, the hydrochemical type was of the $SO_4 \cdot HCO_3 \cdot Cl$-$Na \cdot Ca$ type in SN. Overall, the hydrochemical types of pore and karst water were similar, and of the WR and YR were also close. However, the ion compositions in SN were quite different from the BL, WR, and YR.

Groundwater quality indexes and weights

The groundwater quality indexes (C_1–C_{12}) were sampled and tested from 2015 to 2018 during different water source recharge process. And the data of groundwater quality indexes are shown in Fig. 5. The mean and distribution range of groundwater quality indexes were the smallest in BL, compared with the groundwater quality during WR, YR, and SN recharge. This indicated that the BL of groundwater quality was relatively good, and the changes of BL were small before MAR. Overall, an obvious upward trend appeared in groundwater quality indexes during WR, YR and SN recharge process, and the groundwater quality gradually deteriorated during MAR. Moreover, the weights of the groundwater quality index were determined by AHP and information entropy method, respectively. The combined weights were then calculated according to Eqs. (5)–(7). Finally, the improved matter-element model was developed using combined weights. The combined weights of groundwater quality indexes are shown in Fig. 6.
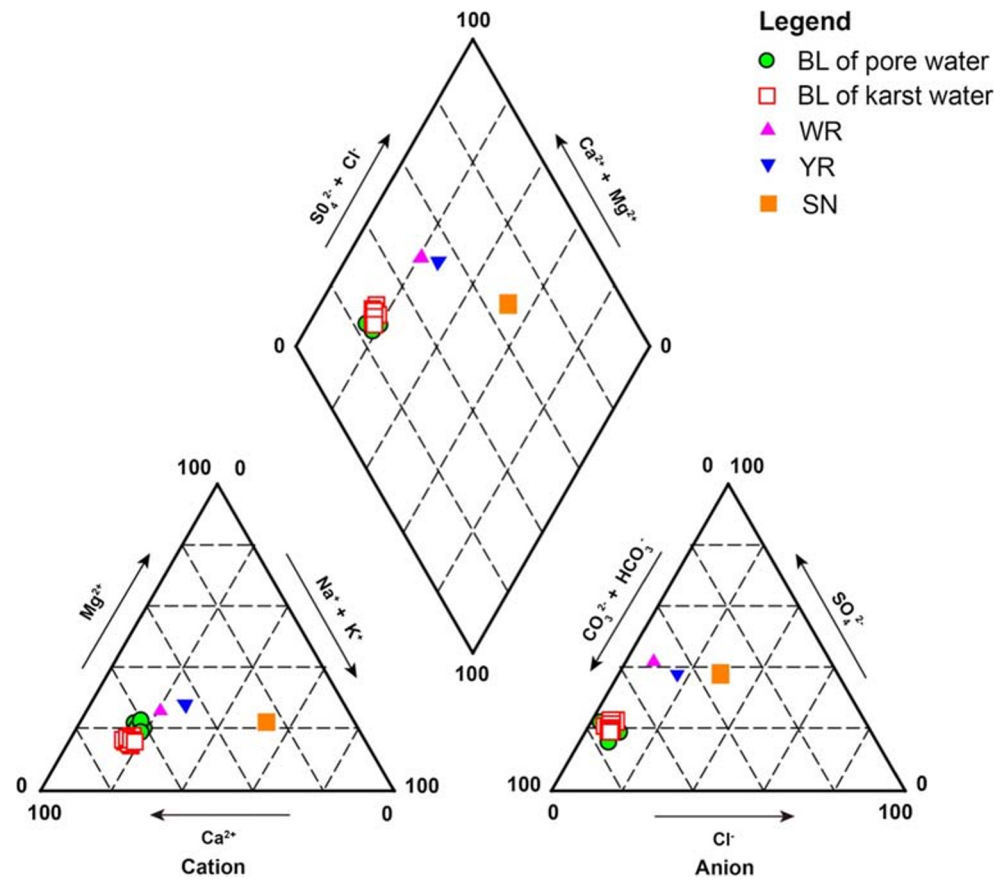
Evaluation of groundwater quality during different water source recharge

The CCD of evaluated matter-element

The CCD of evaluated matter-element related to the classifications standard was calculated during different water source recharge. If the CCD associated with the comprehensive grade was the largest, the evaluation object belonged to this grade. The largest CCD of BL appeared in grades I and II (Fig. 7a). In light of this, the comprehensive grades of BL belonged to grades I and II. The CCD decreased in grade I, and gradually increased in grades II and III, during the WR recharge process (Fig. 7b). It showed that the groundwater quality of monitoring wells was getting worse, and its comprehensive grade was gradually approaching grades II and III. When the YR was used as the source of MAR, the CCD continuously decreased in grade I and increased in grades III and IV (Fig. 7c), meaning that a continuing downward trend occurred in groundwater quality. Compared with BL, WR, and YR, the CCD increased significantly in grades III, IV, and V, during the SN recharge process (Fig. 7d), that is, the comprehensive grade of groundwater quality was changing from grades I and II to grades III, IV and V. Overall, the CCD decreased in grades I and II,

increased in III, IV, and V, when the sources of MAR were WR, YR, and SN.

The comprehensive grade and VE of groundwater quality

The comprehensive grade of groundwater quality could be judged according to the CCD. Meanwhile, the trends in groundwater quality were further revealed by the changes in VE. Based on this, the influence of surface water sources on regional groundwater quality was evaluated in different water source replenishment processes. The higher the comprehensive grades and VE were, the poorer the groundwater quality. As shown in Figs. 8 and 9, the comprehensive grades were all grade II in BL, except monitoring well W6 was grade I. Moreover, the VE ranged from 2.050 to 2.064 with a mean value of 2.056 in porous aquifer (W1–W3) and ranged from 1.940 to 2.005 with a mean value of 1.979 in karst aquifer (W4–W8). In summary, the BL were relatively good, and karst water quality was slightly better than pore water quality.

When the WR was as source of MAR, the comprehensive grades in W1 and W6 were increased to grades III and II, respectively, and the significant changes did not occur in the remaining wells. The VE ranged from 2.184 to 2.220 with a mean value of 2.205 in the porous aquifer, and ranged from
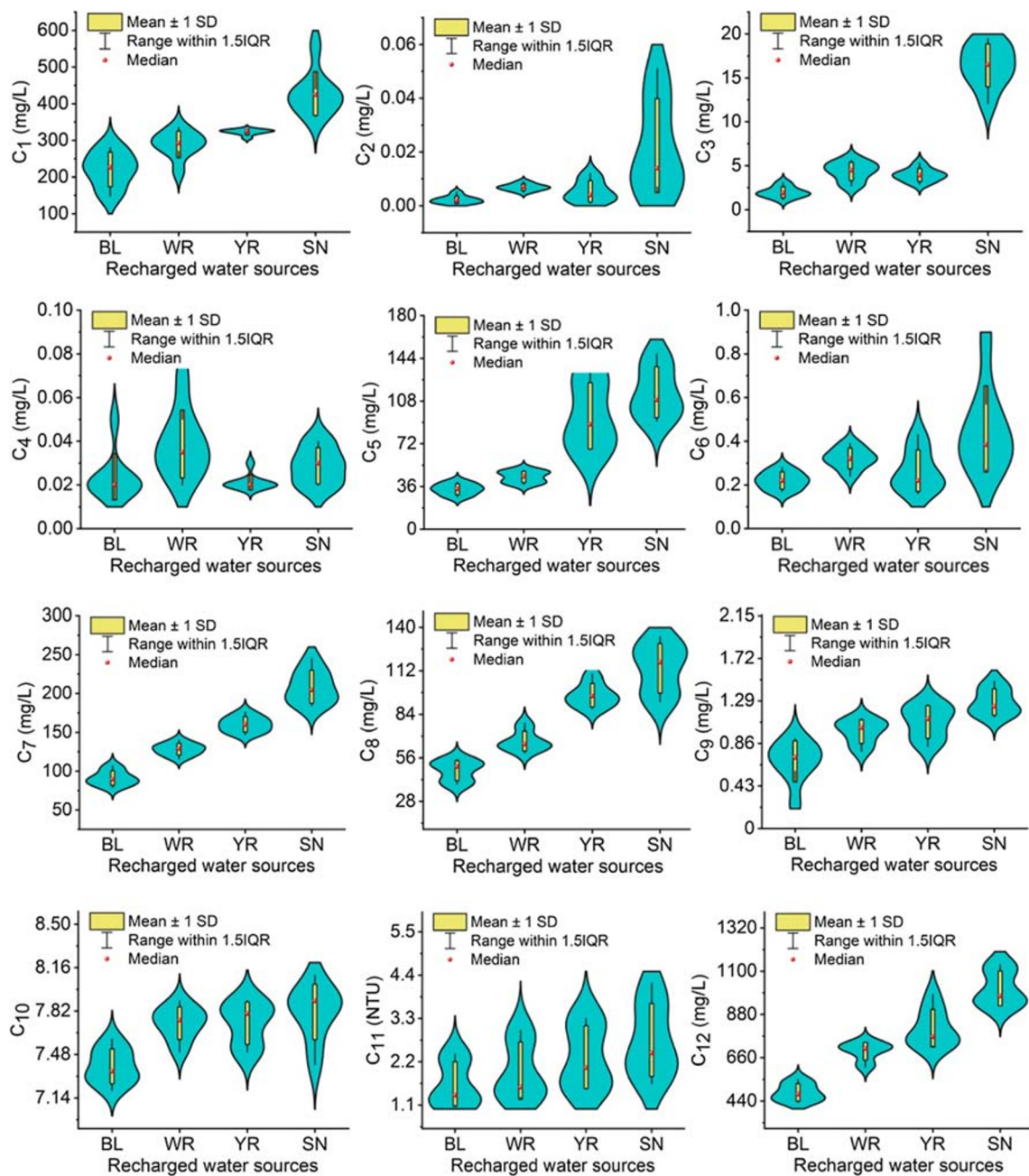
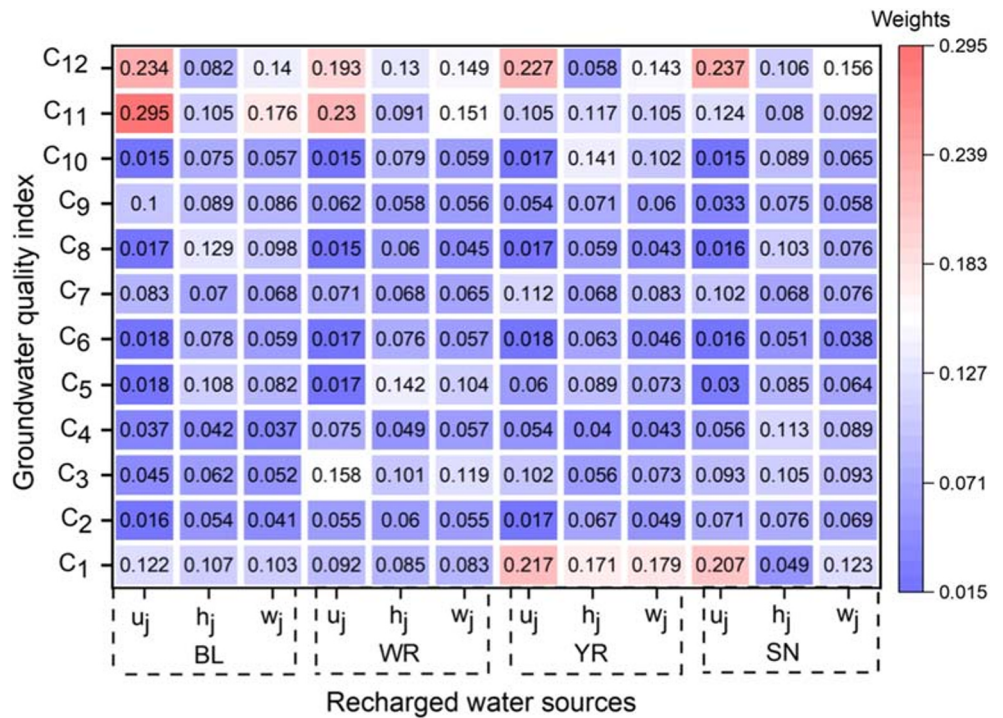**Fig. 5** Groundwater quality indexes

2.054 to 2.118 with a mean value of 2.098 in the karst aquifer. Overall, the VE in pore and karst water quality showed an upward trend after WR recharge, which indicated that a slightly deteriorated trend existed in groundwater quality.

During the YR recharge, the comprehensive grade was grade III in the porous aquifer, and was grade II in the karst aquifer. In addition, the VE ranged from 2.308 to 2.328 with a mean value of 2.321 in porous aquifer, and ranged from 2.208 to 2.258 with a mean value of 2.229 in the karst aquifer. Comparing with the BL and WR, the VE gradually increased. These indicated that the deteriorating trend occurred relative to the

BL during the YR recharge process. Meanwhile, the YR had a greater adverse impact on regional groundwater quality than WR.

The comprehensive grades in porous and karst aquifer were all grade III, when SN was the recharge source. The VE ranged from 2.472 to 2.508 with a mean value of 2.488 in the porous aquifer, and ranged from 2.308 to 2.378 with a mean value of 2.330 in the karst aquifer. The comprehensive grades and VE were the largest during the SN recharge process, compared with WR and YR. These meant that the adverse impact of the SN on regional groundwater quality was greatest relative to WR and YR.

Fig. 6 Weights of groundwater quality index based on different weighting methods. And u_j, h_j, and w_j were the weights obtained by the AHP, information entropy, and ideal solution methods, respectively

Discussion

The dynamic evolution of VE

The dynamic evolution of VE was investigated based on Gaussian kernel density estimation (Fig. 10). A distribution curve with a single peak occurred in BL and double peaks appeared in WR, YR, and SN. The left peak of the bimodal distribution curve represented the karst aquifer (W4–W8), and the right peak was porous medium aquifer (W1–W3). The distribution curve changed from a single peak to double peaks, and the right part of curve extended to the right. In addition, the peak width gradually increased, and both the agglomeration center and right peak had a right-shift trend. These features indicated that the groundwater quality showed a downward trend during different water source recharge. Notably, the difference in groundwater quality between the porous medium aquifer and karst aquifer increased significantly after the

Above knowable, the comprehensive grades and VE of groundwater quality increased in turn and the local groundwater quality showed a deteriorating trend, when the water sources of MAR were WR, YR, and SN, respectively. Meanwhile, the adverse effects of different recharge water sources on regional groundwater quality were SN > YR > WR. Moreover, the VE of pore water quality was slightly larger than that of karst water quality during different water source recharge. This indicated that the karst water quality was better than the pore water quality.

SN recharge. The right-shift distance of the distribution curve in turn was SN > YR > WR > BL. Overall, the adverse effects of different recharge water sources on regional groundwater quality were SN > YR > WR > BL.

The high-risk indexes in groundwater quality

The grades corresponding to the maximum content of groundwater quality index in porous aquifer (W1–W3) during different water source recharge are shown in Fig. 11a. The pore water quality in BL was all grades I and II, except TDS. The contents of TH and NO_3-N increased to grade III after WR recharge. An upward trend occurred in contents of TH, SO_4^{2-}, and TUB after the YR recharge, wherein the TUB increased significantly to grade IV relative to the BL. TH, NO_3-N, SO_4^{2-}, TUB, and TDS all presented an upward trend, when SN was used as the recharge water source. And the contents of TH, TUB, and TDS increased significantly, compared with the BL.

As shown in Fig. 11b, the karst water quality in BL was generally good, and the grades of groundwater quality indexes were all grades I or II, and grade III was not presented. This indicated that the BL of karst water quality were generally better than that of pore water quality. The contents of NO_3-N, NH_4^+, and TDS increased to grade III after WR recharge. TH, NH_4^+, SO_4^{2-}, and TDS showed an upward trend during the YR recharge, the contents of them increased to grade III. During the SN recharge, TH, NO_3-N, NH_4^+, SO_4^{2-}, and TDS displayed a growth trend, wherein the content of TDS had a huge rise to grade IV.
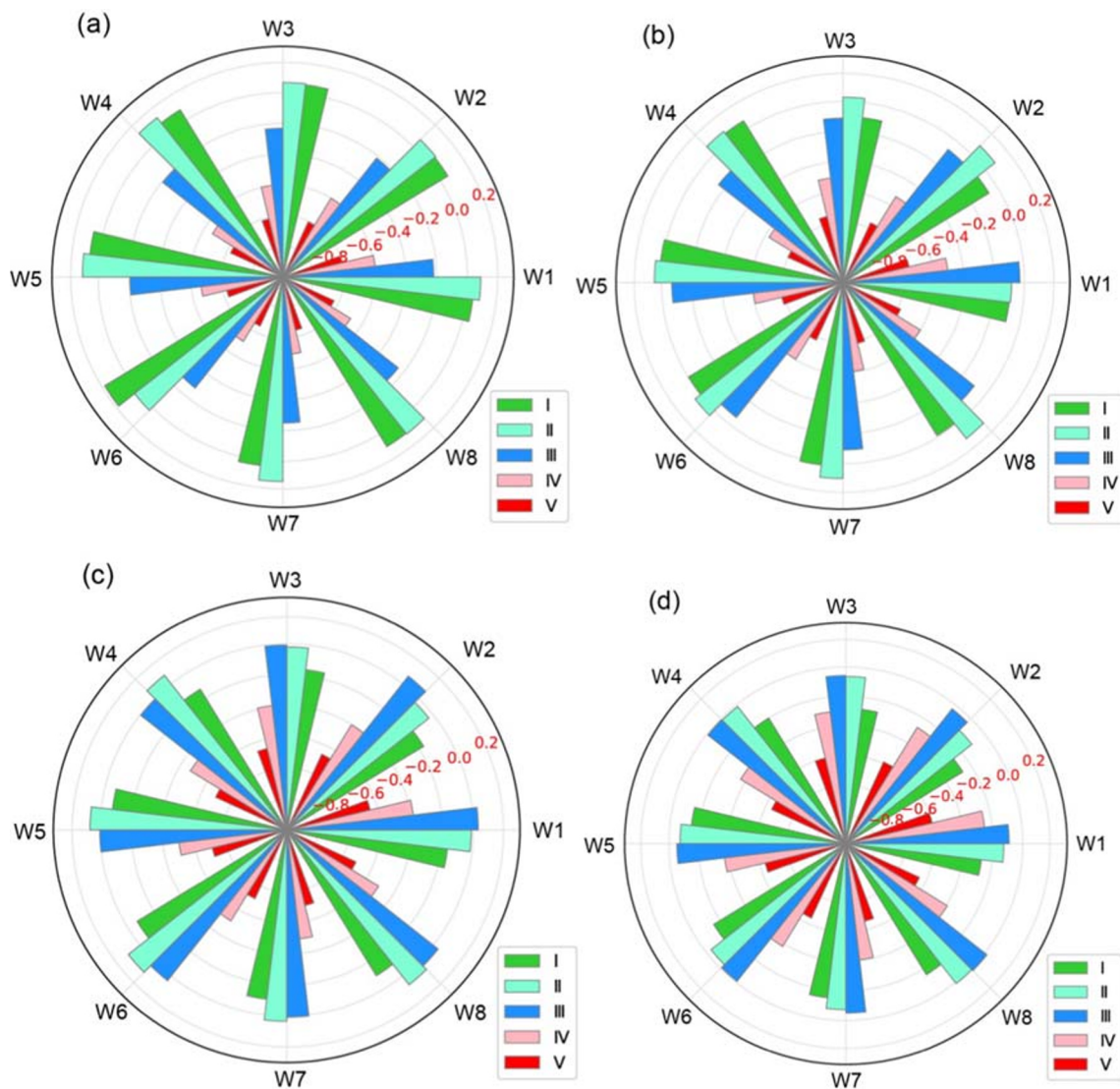
Fig. 7 The CCD of evaluated matter-element. **a** BL. **b** WR. **c** YR. **d** SN

With the rapid socio-economic development, large-scale wastewater and fertilizers generated by production and living were discharged into natural waters, increasing the contents of TH and N in the rivers and lakes (Zhang et al. 2018). Therefore, the content of TH, NO_2-N, NO_3-N, and NH_4^+ in pore and karst water might be increased, when WR, YR, and SN were used as MAR water sources. F^- and COD_{Mn} were less affected by the recharge water sources, the main reason was that the Quaternary sediments (sand and gravel) had a strong adsorption effect on F^- and COD_{Mn} (Li et al. 2017b). Due to the high content of Cl^-, SO_4^{2-}, and Na^+ in YR and SN, these ions in pore and karst water had an upward trend during the YR and SN recharge process. The TUB in groundwater is affected by the suspended solids in the recharged water source. TUB in pore water represented an increasing trend, while that in karst water had not changed significantly after YR and SN recharge. Additionally, an obvious upward trend

appeared in the TDS of pore and karst water, especially after the SN recharge, due to the use of recharge water sources with high TDS.

In summary, a significant increase had occurred in the contents of some groundwater quality indexes during different water source recharge, which might further induce deterioration of regional groundwater quality. According to the aforementioned analysis, TH, NO_3-N, NH_4^+, and TDS were the high-risk indexes of groundwater quality when the WR was used as the recharge water source. The high-risk indexes were TH, NH_4^+, SO_4^{2-}, TUB, and TDS in the YR recharge process. And TH, NO_3-N, NH_4^+, SO_4^{2-}, TUB, and TDS were the high-risk indexes during the SN recharge. Accordingly, these high-risk indexes should be monitored emphatically to reduce the adverse effects on the regional aquifer system, when local groundwater was replenished using the aforementioned surface water sources.

Fig. 8 The comprehensive grades of groundwater quality during different water source recharge
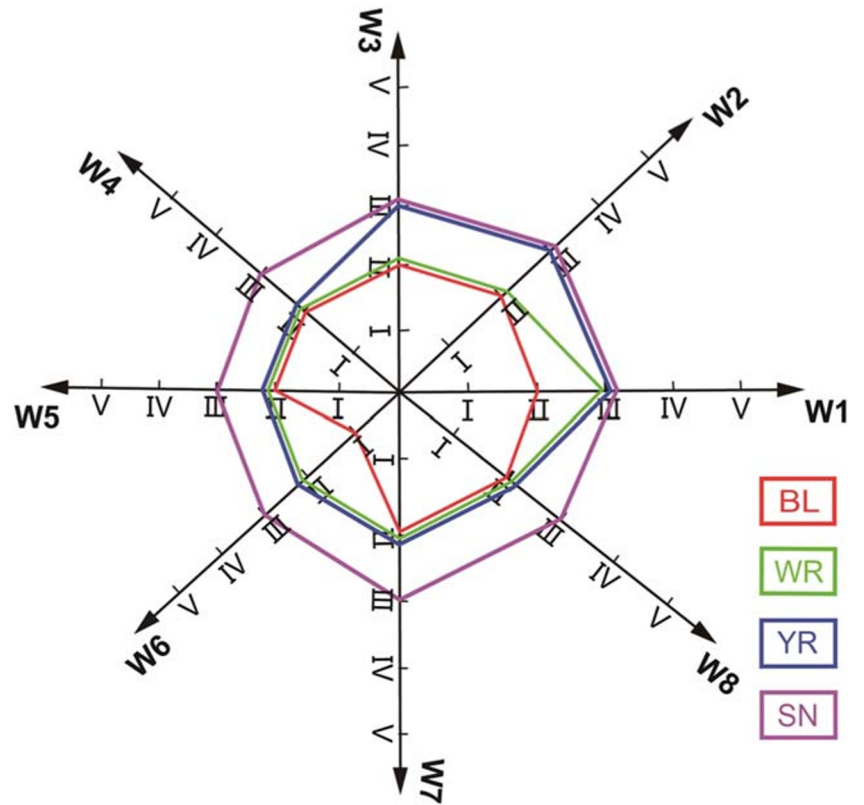

Fig. 9 The VE of groundwater quality during different water source recharge
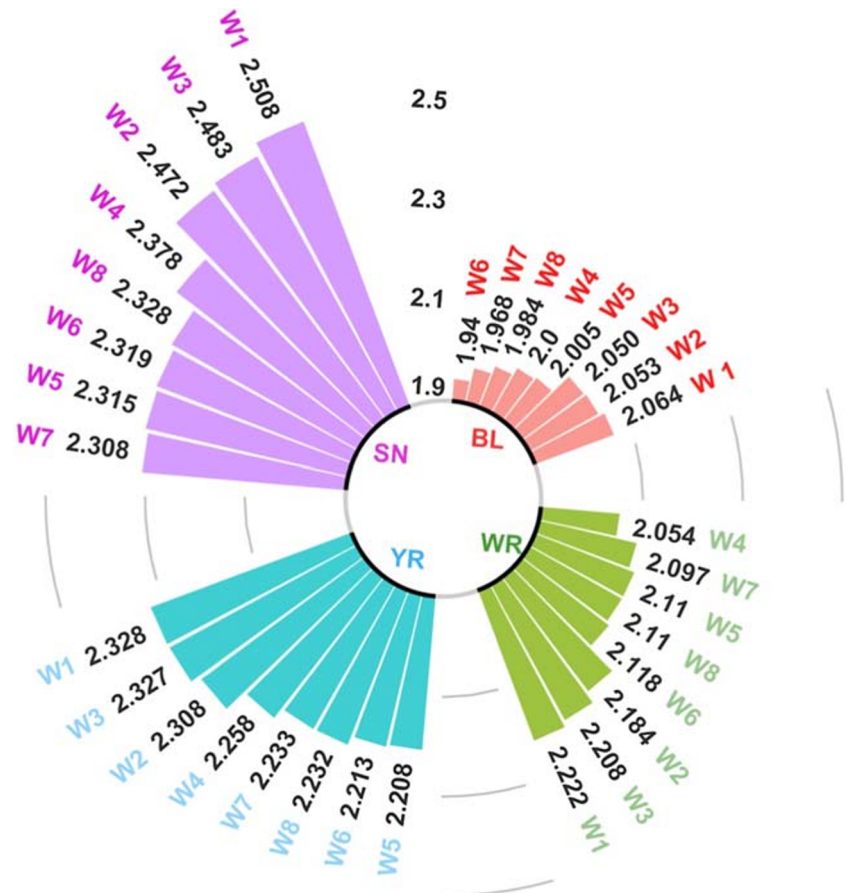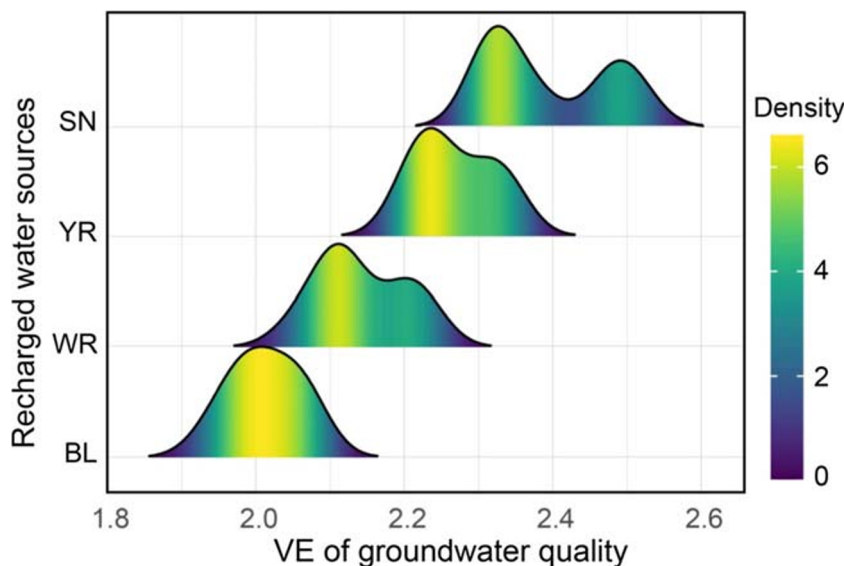
Fig. 10 The Gaussian kernel density estimation of VE

Measures and suggestions

An efficient and low-risk mode for multi-water source recharge was explored by combining the aforesaid results with the existing MAR projects in Jinan. The following measures and suggestions were put forward.

1. The surface water in WR should be used preferentially to replenish the local groundwater resources when the water storage capacity of WR was sufficient. In contrast, if the water storage capacity of WR was insufficient, the YR should be preferentially used as recharge water source. Surface water in SN was considered to use, only when insufficient water supply exists in WR and YR.
2. Whether the replenished water sources were from the WR, the YR, or the SN, the regional groundwater quality will all be affected adversely during the recharge process. These may also lead to the accumulation of some potential high-risk indexes in the aquifer. Therefore, it is necessary to control strictly the proportion of total recharge

quantity to regional groundwater resources. The contents of high-risk indexes in recharge water sources should be reduced as much as possible before recharge, and the abovementioned high-risk indexes in regional groundwater should be monitored emphatically during recharge process.

Study limitations

Due to the restricted spatial variability of the karst aquifer system and availability of data, this study also has some limitations. We only used the groundwater quality data of eight monitoring wells to evaluate the trends in groundwater quality during different water source recharge process, due to the limitation of the number of monitoring wells in the study area. In addition, as a seasonal river, the Yufu River without MAR generated surface runoff only in the flood season (July to August each year), and no surface runoff in the remaining months. During non-flood seasons, the groundwater level

Fig. 11 Grades of the maximum content of groundwater quality index. **a** Grades of groundwater quality index in porous aquifer. **b** Grades of groundwater quality index in karst aquifer
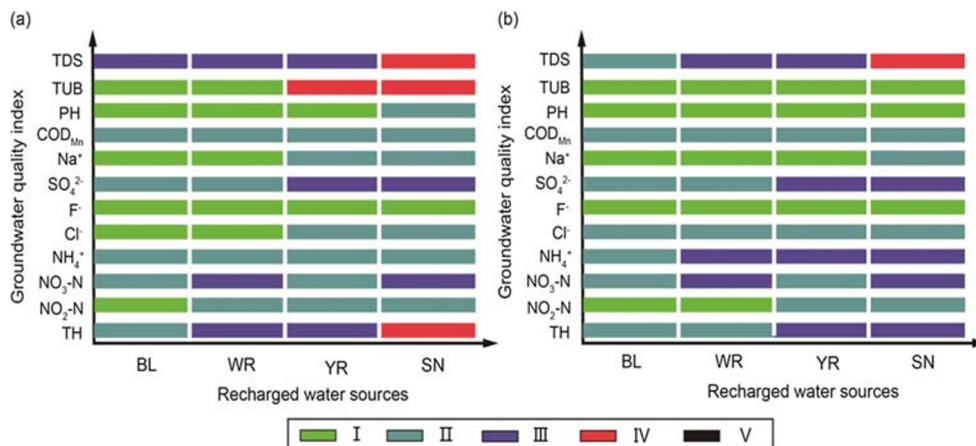
dropped below the bottom of the porous aquifer, and wells in porous medium formation were usually in a dry state. Therefore, this study focused on the investigation of groundwater quality when the groundwater level was higher than the bottom of the porous aquifer during MAR. Possible future researches based on this study include the following: (i) increasing the number of monitoring wells according to the detailed hydrogeological and geophysical investigations; (ii) increasing the types of groundwater quality indexes (such as heavy metals and antibiotics); (iii) adjusting the layout of monitoring wells combining with monitoring sites in pore and karst water; and (iv) investigating the hydrogeochemistry and seasonal variation of groundwater quality based on the regular monitoring of the karst aquifer.

So far, the study area still had not established a MAR scheme to achieve the conjunctive use of surface water and groundwater, and the joint management of water quality and quantity. Therefore, the dynamic changes between water quality and quantity cannot be combined effectively in the MAR with multi-source water. In future researches, the trends in groundwater quality should be investigated dynamically in conjunction with the recharge quantity of different water sources.

Conclusion

In this study, the Yufu River with multiple water sources was used as the research area to carry out large-scale recharge experiments. Under a limited recharged quantity and period, the water quality of groundwater and recharge water source was sampled and tested to study quantitatively the adverse effects of different recharge water sources on local groundwater quality. Meanwhile, the trends in regional groundwater quality were compared and analyzed to investigate the MAR with multi-source water. An improved matter-element model was developed to execute a comprehensive assessment of water quality, and the high-risk indexes in groundwater quality were determined during different water source recharge. The conclusions obtained were as follows.

The hydrochemical type in pore and karst water was of the HCO_3-Ca type before recharge, which indicated that the ion composition was relatively simple, and the BL were relatively good. Furthermore, the hydrochemical type of the WR and YR were relatively close, both of which were of the $HCO_3 \cdot SO_4$-Ca$\cdot$Mg type. The hydrochemical type of the SN was quite different from the BL, WR, and YR, and was of the $SO_4 \cdot HCO_3 \cdot Cl$-Na$\cdot$Ca type. Overall, the water quality of the recharge water source was worse than the BL, and the SN was worst in MAR water sources. Under a limited recharged quantity and period, the adverse effects of different recharge water sources on regional groundwater quality were SN > YR >

WR. Therefore, the long-term and large-scale use of three recharge water sources to replenish groundwater resources might deteriorate the groundwater environment quality and damage the aquifer system.

The combination of improved matter-element model and groundwater quality high-risk indexes provides a new approach to investigate the MAR with multi-source water from multiple perspectives (the overall situation of groundwater quality and the high-risk indexes). We hope this method could be extrapolated to other MAR with multi-source water to optimize the operation of groundwater replenishment and reduce the damage of the recharge water source on the local aquifer system.

Authors' contributions Zhengxian Zhang: methodology, modeling, validation, visualization, writing the original manuscript, and writing review and editing; Weiping Wang: conceptualization, review, and editing.

Data availability All data generated or analyzed during this study are included in this published article (and its supplementary information files).

Compliance with ethical standards

Competing interests The authors declare that they have no conflicts of interest.

Ethical approval and consent to participate Not applicable.

Consent to publish Not applicable.

References

Cai W (1999) Extension theory and its application. Chin Sci Bull 44: 1538–1548

Chen X, Zhang Z-C, Zhang X-N, Chen YQ, Qian MK, Peng SF (2008) Estimation of groundwater recharge from precipitation and evapotranspiration by lysimeter measurement and soil moisture model. J Hydrol Eng 13:333–340

Dermatas D, Mpouras T, Chrysochoou M, Panagiotakis I, Vatseris C, Linardos N, Theologou E, Boboti N, Xenidis A, Papassiopi N, Sakellariou L (2015) Origin and concentration profile of chromium in a Greek aquifer. J Hazard Mater 281:35–46

Dillon P (2005) Future management of aquifer recharge. Hydrogeol J 13: 313–316

Dillon P, Stuyfzand P, Grischek T, Lluria M, Pyne RDG, Jain RC, Bear J, Schwarz J, Wang W, Fernandez E, Stefan C, Pettenati M, van der Gun J, Sprenger C, Massmann G, Scanlon BR, Xanke J, Jokela P, Zheng Y, Rossetto R, Shamrukh M, Pavelic P, Murray E, Ross A, Bonilla Valverde JP, Palma Nava A, Ansems N, Posavec K, Ha K, Martin R, Sapiano M (2019) Sixty years of global progress in managed aquifer recharge. Hydrogeol J 27:1–30

Du X, Wang Z, Ye X (2013) Potential clogging and dissolution effects during artificial recharge of groundwater using potable water. Water Resour Manag 27:3573–3583

Ebrahim GY, Jonoski A, Al-Maktoumi A et al (2016) simulation-optimization approach for evaluating the feasibility of managed aquifer recharge in the Samail Lower Catchment, Oman. J Water Resour Plan Manag 142:05015007

Escalante EF, Sauto JSS, Gil RC (2019) Sites and indicators of MAR as a successful tool to mitigate climate change effects in Spain. Water 11: 1943

Fernández Escalante E (2015) Practical management to minimize the effects of clogging in managed aquifer recharge wells at two sites in the Guadiana Basin, Spain. J Hydrol Eng 20:B5014002

Fiorillo F, Pagnozzi M, Stevanović Z, Ventafridda G (2019) Main hydrological features and recharge analysis of the Caposele Spring catchment, southern Italy. Acta Carsologica 48. https://doi.org/10.3986/ac.v48i1.6738

Ganot Y, Holtzman R, Weisbrod N, Nitzan I, Katz Y, Kurtzman D (2017) Monitoring and modeling infiltration–recharge dynamics of managed aquifer recharge with desalinated seawater. Hydrol Earth Syst Sci 21:4479–4493

Gao Y, Tian Y (2018) Groundwater chemical characteristics in the upper reaches of the Langmaoshan Reservoir, Shandong. Resour Sci 40: 359–368 (in Chinese)

Gao Z, Xu J, Wang S et al (2014) The distribution characteristics and hydrogeological significance of trace elements in karst water, Jinan, China. Earth Sci Front 21(4):135–146 (in Chinese)

Gong Y, Wang X, Hu B et al (2016) Groundwater contributions in water-salt balances of the lakes in the Badain Jaran Desert, China. J Arid Land 8:694–706

Hou W, Sun S, Wang M, Li X, Zhang N, Xin X, Sun L, Li W, Jia R (2016) Assessing water quality of five typical reservoirs in lower reaches of Yellow River, China: using a water quality index method. Ecol Indic 61:309–316

Jiao F, Ren L, Wang X, Liu W (2017) Pollution characteristics and potential ecological risk assessment of metals in the sediments of Xiaoqing River, Jinan. Environ Sci Pollut Res 24:15001–15011

Kang F, Jin M, Qin P (2011) Sustainable yield of a karst aquifer system: a case study of Jinan springs in northern China. Hydrogeol J 19:851–863

Leonard R, Mankad A, Alexander K (2015) Predicting support and likelihood of protest in relation to the use of treated stormwater with managed aquifer recharge for potable and non-potable purposes. J Clean Prod 92:248–256

Li B, Yang G, Wan R, Hörmann G (2017a) Dynamic water quality evaluation based on fuzzy matter–element model and functional data analysis, a case study in Poyang Lake. Environ Sci Pollut Res 24:19138–19148

Li F, Wang W, Xu Q et al (2017b) Assessment of water quality risk from karst aquifer recharge with multi-source water in the Yufuhe river, Jinan. Carsologica Sin 36:751–758 (in Chinese)

Liang X, Zhan H, Zhang Y-K (2018) Aquifer recharge using a vadose zone infiltration well. Water Resour Res 54:8847–8863

Liu D, Zou Z (2012) Water quality evaluation based on improved fuzzy matter-element method. J Environ Sci 24:1210–1216

Liu Y, Zhang Z, Zhang F (2019) Challenges for water security and sustainable socio-economic development: a case study of industrial, domestic water use and pollution management in Shandong, China. Water 11:1630

Liu Y, Yang L, Jiang W (2020a) Qualitative and quantitative analysis of the relationship between water pollution and economic growth: a case study in Nansi Lake catchment, China. Environ Sci Pollut Res 27:4008–4020

Liu Y, Yang L, Jiang W (2020b) Coupling coordination and spatiotemporal dynamic evolution between social economy and water

environmental quality – a case study from Nansi Lake catchment, China. Ecol Indic 119:106870

Luo Q, Yang Y, Qian J, Wang X, Chang X, Ma L, Li F, Wu J (2020) Spring protection and sustainable management of groundwater resources in a spring field. J Hydrol 582:124498

Malík P, Michalko J, Pažická A, Máša B, Stankovič J (2020) Detailed water quality monitoring at various points of the Krásnohorská Cave system (Slovakia). In: Bertrand C, Denimal S, Steinmann M, Renard P (eds) Eurokarst 2018, Besançon. Springer International Publishing, Cham, pp 199–212

Mankad A, Walton A, Alexander K (2015) Key dimensions of public acceptance for managed aquifer recharge of urban stormwater. J Clean Prod 89:214–223

Massmann G, Sültenfuß J (2008) Identification of processes affecting excess air formation during natural bank filtration and managed aquifer recharge. J Hydrol 359:235–246

Missimer TM, Guo W, Woolschlager J, Maliva RG (2017) Long-term managed aquifer recharge in a saline-water aquifer as a critical component of an integrated water scheme in Southwestern Florida, USA. Water 9:774

Page D, Dillon P, Vanderzalm J, Toze S, Sidhu J, Barry K, Levett K, Kremer S, Regel R (2010) Risk assessment of aquifer storage transfer and recovery with urban stormwater for producing water of a potable quality. J Environ Qual 39:2029–2039

Parker LV, Clark CH (2004) Study of five discrete-interval-type ground water sampling devices. Groundw Monit Remediat 24:111–123

Qi X, Wang Y, Yang L et al (2016) Time lags variance of groundwater level response to precipitation of Jinan karst spring watershed in recent 50 years. Carsologica Sin 35:384–393 (in Chinese)

Rodríguez Escales P-F, Canelles Garcia A, Sánchez Vila FJ, Folch Sancho A (2018) A risk assessment methodology to evaluate the risk failure of managed aquifer recharge in the Mediterranean Basin. Hydrol Earth Syst Sci 22:3213–3227

Rodríguez-Escales P, Fernàndez-Garcia D, Drechsel J, Folch A, Sanchez-Vila X (2017) Improving degradation of emerging organic compounds by applying chaotic advection in managed aquifer recharge in randomly heterogeneous porous media. Water Resour Res 53: 4376–4392

Tang Q-Y, Zhang C-X (2013) Data Processing System (DPS) software with experimental design, statistical analysis and data mining developed for use in entomological research. Insect Sci 20:254–260

Urrutia J, Herrera C, Custodio E, Jódar J, Medina A (2019) Groundwater recharge and hydrodynamics of complex volcanic aquifers with a shallow saline lake: Laguna Tuyajto, Andean Cordillera of northern Chile. Sci Total Environ 697:134116

Wang J-J, Jing Y-Y, Zhang C-F, Zhao J-H (2009) Review on multi-criteria decision analysis aid in sustainable energy decision-making. Renew Sust Energ Rev 13:2263–2278

Wang J, Jin M, Jia B, Kang F (2015a) Hydrochemical characteristics and geothermometry applications of thermal groundwater in northern Jinan, Shandong, China. Geothermics 57:185–195

Wang W, Page D, Zhou Y et al (2015b) Roof runoff replenishment of groundwater in Jinan, China. J Hydrol Eng 20: B5014005

Wang J, Jin M, Lu G, Zhang D, Kang F, Jia B (2016) Investigation of discharge-area groundwaters for recharge source characterization on different scales: the case of Jinan in northern China. Hydrogeol J 24:1723–1737

Wang J, Wang J, Jin M (2017a) Hydrochemical characteristics and formation causes of karst water in Jinan spring catchment. J China U Geosci 42:821–831 (in Chinese)

Wang X, Wang C, Wang B, Liu S, Song J (2017b) Protection of urban features during urbanization based on the roles of springs in Jinan. Chin J Popul Resour Environ 15:93–102

Wang G-F, Wu Y-X, Lu L, Li G, Shen JS (2019) Investigation of the geological and hydrogeological environment with relation to metro

system construction in Jinan, China. Bull Eng Geol Environ 78: 1005–1024

Werner AD, Zhang Q, Xue L, Smerdon BD, Li X, Zhu X, Yu L, Li L (2013) An initial inventory and indexation of groundwater mega-depletion cases. Water Resour Manag 27:507–533

Wu Q, Xu H (2005) A three-dimensional model and its potential application to spring protection. Environ Geol 48:551–558

Xie L (2017) Advanced engineering and technology III: Proceedings of the 3rd Annual Congress on Advanced Engineering and Technology (CAET 2016), Hong Kong, 22-23 October 2016. CRC Press

Xing L, Huang L, Hou X, Yang L, Chi G, Xu J, Zhu H (2018) Groundwater hydrochemical zoning in inland plains and its genetic mechanisms. Water 10:752

Xu Z, Hu BX, Davis H, Kish S (2015) Numerical study of groundwater flow cycling controlled by seawater/freshwater interaction in a coastal karst aquifer through conduit network using CFPv2. J Contam Hydrol 182:131–145

Ye X, Cui R, Du X et al (2019) Mechanism of suspended kaolinite particle clogging in porous media during managed aquifer recharge. Groundwater 57:764–771

Yin D, Shu L, Chen X, Wang Z, Mohammed ME (2011) Assessment of sustainable yield of karst water in Huaibei, China. Water Resour Manag 25:287–300

Yin X, Wang Q, Feng W (2017) Hydro-chemical and isotopic study of the karst spring catchment in Jinan. Acta Geol Sin 91:1651–1660 (in Chinese)

Yu H, Huang G, Wu C (2014) Application of the stormwater management model to a piedmont city: a case study of Jinan City, China. Water Sci Technol 70:858–864

Zhang Z, Li Y (2020) Coupling coordination and spatiotemporal dynamic evolution between urbanization and geological hazards–a case study from China. Sci Total Environ 728:138825. https://doi.org/10.1016/j.scitotenv.2020.138825

Zhang D, Shu J, Sun J (2017a) Observed deformation characteristics of a deep excavation for the spring area in Jinan, China. J Mt Sci 14:581–594

Zhang L, Qin X, Tang J, Liu W, Yang H (2017b) Review of arsenic geochemical characteristics and its significance on arsenic pollution studies in karst groundwater, Southwest China. Appl Geochem 77:80–88

Zhang Z, Wang W, Qu S, Huang Q, Liu S, Xu Q, Ni L (2018) A new perspective to explore the hydraulic connectivity of karst aquifer system in Jinan spring catchment, China. Water 10: 1368

Zhu X, Wu J, Nie H, Guo F, Wu J, Chen K, Liao P, Xu H, Zeng X (2018) Quantitative assessment of the impact of an inter-basin surface-water transfer project on the groundwater flow and groundwater-dependent eco-environment in an oasis in arid northwestern China. Hydrogeol J 26:1475–1485